Nanoliter droplet coalescence in air by directional acoustic ejection

Chuang-Yuan Lee,[a] Hongyu Yu, and Eun Sok Kim
Department of Electrical Engineering-Electrophysics, University of Southern California, 3737 Watt Way, PHE 535, Los Angeles, California 90089

(Received 13 April 2006; accepted 19 October 2006; published online 30 November 2006)

This letter presents a controlled coalescence of nanoliter liquid droplets in air by acoustic directional ejections. An asymmetrical electric field is created within a piezoelectric transducer to produce lopsided acoustic waves, which are focused (through a lens based on the innate impedance mismatch between solid and gas) onto a spot on the liquid surface. The focused acoustic beam is shown to obliquely eject 80-μm-diameter droplets at a traveling speed of 2.3 m/s. Up to four such obliquely ejected droplets coalesce in air into a single droplet, which then continue to travel, rotating at 16 000 rad/s and producing effective micromixing in air. © *2006 American Institute of Physics*. [DOI: 10.1063/1.2398886]

The interest in creating and controlling microdroplets is growing rapidly, driven by emerging applications in biomedicine, chemistry, and pharmaceutics.[1,2] Existing droplet generation methods fall into two general categories—contact pin dispensing and noncontact inkjet dispensing. Pin-based dispensing has gained extensive attention for printing deoxyribonucleic acid and protein microarrays.[3,4] However, the pin is subject to clogging and the chip coating is prone to damages because the liquid-loaded pin contacts the chip surface.[5]

Alternatively, inkjet dispensing is a noncontact method to shoot out microdroplets onto a chip surface. Thermal and piezoelectric actuations are the two most widespread mechanisms and have been broadly reported for mass spectrometer analysis,[6] metal deposition,[7] tissue engineering,[8] and printing polymer light-emitting diodes.[9] In the thermal method, droplets are ejected from a nozzle through the growth and collapse of vapor bubbles generated by a heater. In the piezoelectric method, a hydrostatic pressure produced by the mechanical bending of a piezoelectric unimorph (or by a flextensional ultrasound transducer[10]) forms a droplet at the nozzle. Both methods suffer from the inherent tendency of nozzle clogging. In addition, droplets can be ejected only in a direction perpendicular to the nozzle surface.

Nozzleless dispensing is possible with acoustic actuations.[11] An acoustic beam focused on the liquid surface can overcome the surface tension and expel liquid droplets from an open space without any nozzle. A variety of acoustic focusing mechanisms have been reported. Fresnel lens has the advantage of being planar, but the lens thicknesses are tightly restrained for the desired 180° phase difference between the waves traveling through the liquid and the lens.[12] Surface acoustic waves have also been utilized for droplet ejections.[13]

In this letter, we introduce an effective focusing scheme (which we call "lens with air reflectors" or LWARs) by utilizing the innate acoustic impedance mismatch between solid and gas and report the coalescence of liquid droplets in air resulting from acoustic directional ejections. A lead zirconate titanate (PZT) transducer (PSI-5A4E, Piezo Systems) with both top and bottom nickel electrodes patterned into a quadrant was used to produce directional ejections [Fig. 1(a)]. Asymmetric acoustic fields were generated from the "pie-shaped" sector electrodes, in contrast to symmetric acoustic fields generated from circular electrodes. The electric field applied across the thickness of the piezoelectric PZT causes the PZT to vibrate, producing acoustic waves. Since the vibrations happen only at the regions covered with the sector electrodes, uneven acoustic pressure distributions are produced at the liquid surface. Simulations show that as the sector angle decreases, the vertical particle displacement at the liquid surface becomes less intensified, while the relative lateral displacement becomes larger (Table I). It has been experimentally shown that the ejection becomes more tilting as the sector angle gets smaller. However, a smaller sector angle means a smaller actuation area and weaker acoustic-power generation. Thus it requires a larger minimum pulse width for stable ejections. Though it has been experimentally observed that the ejection stability and droplet size are sen-

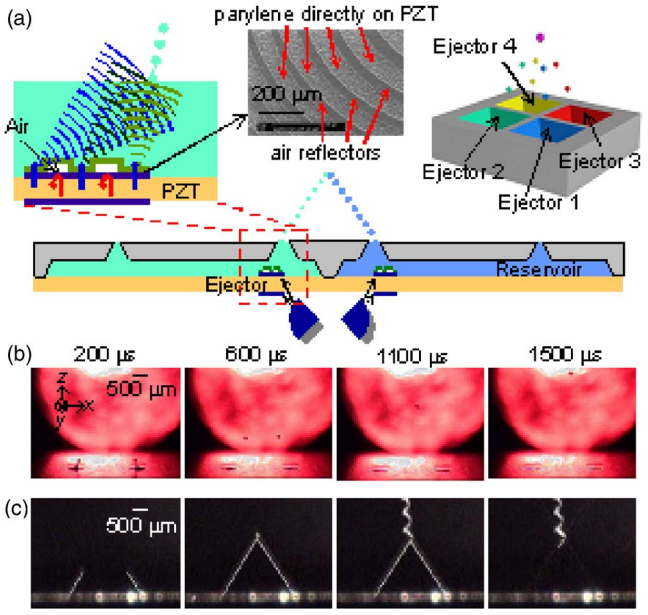

FIG. 1. (a) Schematic diagram of the directional acoustic ejector array. (b) Optical micrographs with strobe (ejectors 1 and 2 activated). (c) Optical micrographs without strobe. The shutter-opening time of the charge-coupled device camera (SONY SSC-DC54A) was set to 2 ms to record the images.

[a]Author to whom correspondence should be addressed; FAX: 1-213-740-8677; electronic mail: chuangy1@usc.edu

TABLE I. Particle displacements on the liquid surface for different electrode patterns.

Apex angle of sectored electrode (deg)	360	270	180	90
Normalized particle displacement	8.1	6.4	4.4	2.0
Ratio of lateral to vertical particle displacement	0	0.16	0.37	0.59

sitive to the pulse width, the pulse width effect on acoustic ejection remains unclear for lack of theory.[10] In the case of directional ejection, we found that the directionality is also a function of pulse width and that a larger pulse width would result in a less oblique ejection angle.

By taking advantage of the fact that air has an acoustic impedance much smaller than any solids, LWAR provides a method to focus the acoustic waves. Due to impedance mismatch, the acoustic waves are mostly reflected at the transducer-air interface. To ensure efficient acoustic transmission, the lens structure was built with parylene (that is biocompatible), because its impedance is between that of the liquid medium and the transducer. As a result, the acoustic waves were transmitted into liquid through the parylene but reflected by the air pockets. We patterned the lens into Fresnel half-wave bands (with the kth radius given by $\sqrt{k\lambda(F+k\lambda/4)}$, where λ and F are the acoustic wavelength and the lens focal length, respectively[14]) so that the transmitted acoustic pressure was magnified at the liquid surface due to constructive interference.

Four such ejectors, integrated with their own 800-μm-deep (matching the lens focal length) reservoirs, were arrayed on a single chip to target one spot in the center with multiple liquids. By applying pulses of an 18 MHz (the fundamental thickness-mode resonance frequency of the 127-μm-thick PZT) sinusoidal signal to the ejector, we were able to digitally regulate the ejection for one droplet per pulse at an ejection rate up to 10 kHz. We first actuated ejectors 1 and 2 using water as the liquid [Fig. 1(b)]. The ejectors were driven with ± 80 $V_{p,p}$ pulses. The pulse width and the pulse repetition frequency (PRF) were 16 μs and 60 Hz, respectively. Two 80-μm-diameter spherical droplets broke off simultaneously from their own bulk liquids 200 μs after the rising edge of a pulse. They then approached each other with an ejection angle of 60° at a speed of 2.3 m/s. At around 1100 μs, they arrived at the same place and coalesced into one larger ellipsoid. The coalesced droplet kept on traveling in air with no velocity along the $\hat{x}$ direction [Fig. 1(c)].

As two droplets collide, bounce will occur if the droplets' surfaces undergo a flattening deformation without making contact due to a thin air layer between the droplets. The colliding droplets will coalesce when the air layer thickness reaches a critical value, typically of the order of 100 Å.[15] The droplets may coalesce permanently or temporarily, depending on the collisional kinetic energy (CKE) and impact parameter b which is defined as the distance from the center of one droplet to the relative velocity vector placed on the center of the other droplet as they collide. The total collisional energy E_{TC}, equal to CKE plus surface-energy reduction, is dissipated through the deformations and rotations of the droplets. The rotational energy of the coalesced droplet is calculated as $E_r=(1/2)I\omega^2$, where I and ω are the moment of inertia and angular frequency, respectively. In temporary coalescence, E_{TC} is so large that the coalesced droplet undergoes catastrophic fragmentation into numerous small droplets.[16] According to experimental data, whether droplets bounce, coalescence, or fragment is typically predictable in the (b, We), plane, where the Weber number is defined as $We=\rho(D_1+D_2)|\mathbf{v}_1-\mathbf{v}_2|^2/2\sigma$, where ρ is the liquid density, σ is the surface tension, D_1 and D_2 are the diameters, and $|\mathbf{v}_1-\mathbf{v}_2|$ is the relative velocity of the droplets.

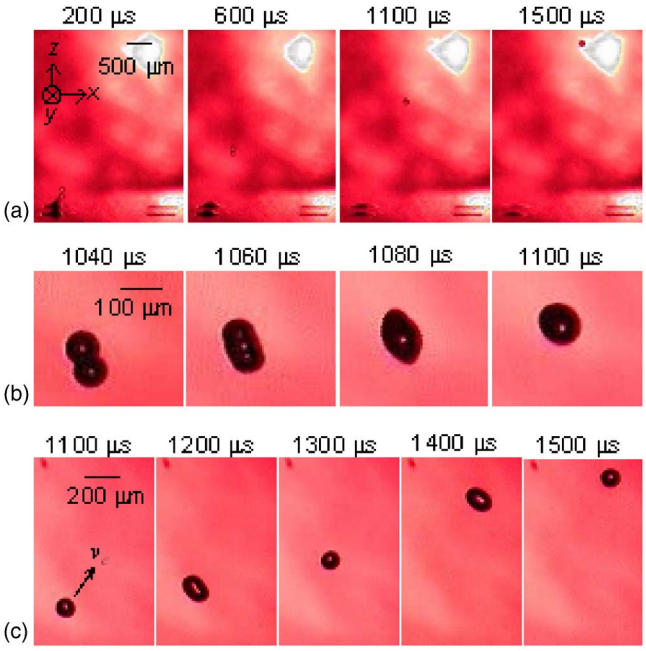

FIG. 2. Optical micrographs of the ejection process (ejectors 2 and 4 activated). (a) Overview pictures. (b) Detailed coalescence sequence. (c) Rotations of the traveling coalesced droplet with a periodicity of 400 μs.

Using $D_1=D_2=80$ μm, $|\mathbf{v}_1-\mathbf{v}_2|=1.7$ m/s, $b=50$ μm, $\sigma=0.073$ N/m, $\rho=1000$ kg/m^3, and $\omega=16\,000$ rad/s, we calculate We, CKE, E_{TC}, and E_r to be 3.2, 0.19 nJ, 0.79 nJ, and 0.07 nJ, respectively. With $b=0.6D$ and We=3.2, the collision falls into the stable coalescence region.[15] The droplet size, relative velocity, and angular frequency are in good quantitative agreement with other droplet collision studies on atmospheric raindrop formation and spray combustion.[15,17] In the work of Adam *et al.*, as two 60 μm water droplets collide with a relative velocity of 2 m/s, the coalesced droplet rotates at 15 300 rad/s. However, that particular experiment required a large apparatus with two ejectors that are manually mounted.

The ejection sequences of ejectors 2 and 4 show the coalescence from another angle (Fig. 2). After coalescence, the coalesced prolate spheroid (cigar-shaped ellipsoid) droplet rotated with a periodicity of 400 μs, as its airborne travel continued [Fig. 2(c)].

The rotating characteristics of the coalesced droplet can be applied to micromixing. To illustrate the mixing effect, one ink and one water droplet were ejected for coalescence in air, and we examined the droplets collected on a glass slide placed 2 cm above the device (Fig. 3). The number of revolutions N_r (at a traveling distance S) is calculated as $N_r=\omega S/2\pi v_c$, where v_c is the proceeding velocity after coalescence. With $\omega=16\,000$ rad/s and $v_c=2.1$ m/s, the coalesced droplet was mingled swiftly by rotating about 25 revo before it reached the glass slide. The droplet landing position could be controlled within 80 μm. To quantify the mixing performance, the mixing index is calculated as

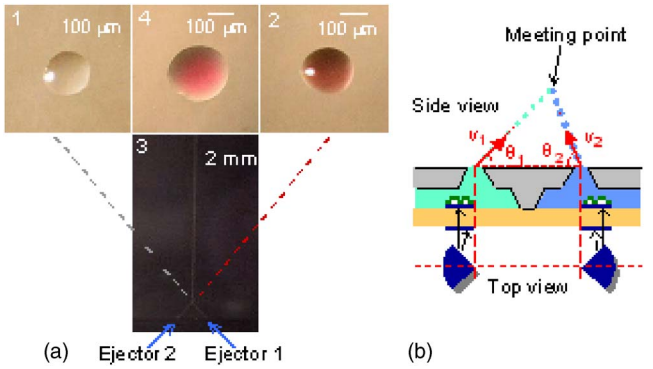

FIG. 3. (a) Optical micrographs of the water, ink, and mixed droplets ejected onto a glass slide. Water was used for ejector 1, while red ink was used for ejector 2. For comparison, one water droplet (~0.27 nl) was first ejected by ejector 1 (image 1) and then one ink droplet was ejected by ejector 2 (image 2). Finally, one water and one ink droplet were simultaneously ejected (image 3). The coalesced droplet continued traveling until it was collected on the glass slide (image 4). (b) Schematic diagram showing that the trajectories of any two different liquid droplets intersect in air.

$$\text{Mixing index} = \sqrt{\frac{1}{N}\sum_{k=1}^{N}\left(\frac{c_k - \bar{c}}{\bar{c}}\right)^2}, \quad (1)$$

where c_k and $\bar{c}$ are the color index at pixel k and the average of N pixels,[18] respectively. We compared the time required to mix the same liquid volume by rotation in air and by diffusion. To carry out the diffusion experiment without evaporation, droplets were ejected inside the oil and mixed by diffusion. It was observed that diffusion took 6 s to reach the mixing index of 0.13 while rotation in air took less than 0.05 s to reach 0.11, a 120 times reduction in time. In addition, the trajectories of any two different liquid droplets will intersect in air as long as the two ejectors are placed symmetrically as shown in Fig. 3(b). Thus even liquids with different viscosities and densities can meet at the same spot by controlling the delay time between the actuation pulses to the ejectors.

To demonstrate that more than two droplets can be merged in air, we simultaneously actuated four ejectors. Driven with $\pm 80\ V_{P.P.}$ pulses of 30 μs pulse width and 60 Hz PRF, the four ejected droplets moved toward the center with an angle of 75° and joined together in air after 1800 μs (Fig. 4). For coalescence of two droplets, 80% of the devices can eject droplets for coalesce. It becomes harder to coalescence three or four droplets in air. However, for the working ejectors, the coalescence process is 100% repeatable.

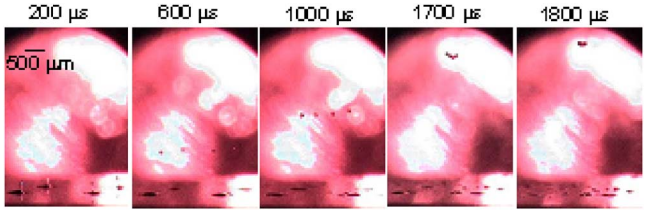

FIG. 4. Optical micrographs of the ejection process when four ejectors were activated.

In conclusion, we have demonstrated a droplet dispensing method capable of targeting the same spot in air, with combinations of different reagents. Because of its high throughput, positional accuracy, reproducibility, and low susceptibility to clogging, this digital fluid manipulation by directional droplet ejections will be useful not only for inkjet printing but also for various biochemical applications, ranging from drug screenings to combinatorial chemistry.

This work was supported by National Science Foundation (NSF) under Grant No. ECS-0310622.

[1] M. Schena, D. Shalon, R. W. Davis, and P. O. Brown, Science **270**, 467 (1995).
[2] J. L. DeRisi, V. R. Iyer, and P. O. Brown, Science **278**, 680 (1997).
[3] D. J. Duggan, M. Bittner, Y. Chen, P. Meltzer, and J. Trent, Nat. Genet. **21**, 10 (1999).
[4] G. MacBeath and S. L. Schreiber, Science **289**, 1760 (2000).
[5] H. B. Hsieh, J. Fitch, D. White, F. Torres, J. Roy, R. Matusiak, B. Krivacic, B. Kowalski, R. Bruce, and S. Elrod, J. Biomol. Screening **9**, 85 (2004).
[6] T. Laurell, J. Nilsson, and G. Marko-Varga, J. Chromatogr., B: Biomed. Sci. Appl. **752**, 217 (2001).
[7] G. G. Rozenberg, E. Bresler, S. P. Speakman, C. Jeynes, and J. H. G. Steinke, Appl. Phys. Lett. **81**, 5249 (2002).
[8] T. Xu, J. Jin, C. Gregory, J. J. Hickman, and T. Boland, Biomaterials **26**, 93 (2005).
[9] T. R. Hebner, C. C. Wu, D. Marcy, M. L. Lu, and J. Sturm, Appl. Phys. Lett. **72**, 519 (1998).
[10] G. Percin, T. S. Lundgren, and B. T. Khuri-Yakub, Appl. Phys. Lett. **73**, 2375 (1998).
[11] S. A. Elrod, B. Hadimioglu, B. T. Khuri-Yakub, E. G. Rawson, E. Richley, C. F. Quate, N. N. Mansour, and T. S. Lundgren, J. Appl. Phys. **65**, 3441 (1989).
[12] S. C. Chan, M. Mina, S. S. Udpa, L. Udpa, and W. Lord, IEEE Trans. Ultrason. Ferroelectr. Freq. Control **43**, 670 (1996).
[13] U. Demirci, Appl. Phys. Lett. **88**, 144104 (2006).
[14] D. Huang and E. S. Kim, J. Microelectromech. Syst. **10**, 442 (2001).
[15] M. Orme, Prog. Energy Combust. Sci. **23**, 65 (1997).
[16] T. B. Low and R. List, J. Atmos. Sci. **39**, 1591 (1982).
[17] J. R. Adam, N. R. Lindelad, and C. D. Hendricks, J. Appl. Phys. **39**, 5173 (1968).
[18] L.-H. Lu, K. S. Ryu, and C. Liu, J. Microelectromech. Syst. **11**, 462 (2002).